Geotechnical and Structural Engineering for Old Historic Buildings

Kari Chr. Avellan[1], Kirsi Vaali[2] and Erika Belopotocanova[3]

[1]*D. Sc. (Tech), KAREG Consulting Engineers, Helsinki, Finland, email: kari.avellan@kareg.com*

[2]*Associate Prof., PhD., SelexLab Oy, Luoma, Finland, email: kirsi.vaali@selexlab.fi*

[3]*Engineer, KAREG Consulting Engineers, Helsinki, Finland, email: erika.belopotocanova@kareg.com*

ABSTRACT

The preservation of historic buildings requires strengthening and underpinning of foundations whose geometry, condition, and geotechnical environment are only partially known. Successful rehabilitation needs an integrated geotechnical and structural engineering approach combined with practical construction experience. This paper presents two case studies involving the strengthening of historic masonry structures founded on problematic soils. The first case concerns Alexander Street in Helsinki, Finland, a building dating from approximately 1840. Investigations showed that part of the structure was founded on silty clay that continued to deform under loading despite more than 150 years service. The corridor foundations were successfully underpinned using as shoring drilled and grouted steel piles for new reinforced concrete piers. The second case, St. John's Church in Tartu, Estonia, was constructed in the late thirteenth century. The church foundations consisted of masonry resting on timber rafts over loose sandy silt. Long-term settlement and groundwater lowering required extensive underpinning of the tower, walls, and columns using jacked piles, drilled spiral piles, and piled raft foundations. In addition, the destroyed Line B section of the church was reconstructed. A practical design method based on Lower Bound Theorem of Plasticity is presented for the design of floating piled strip foundations and for soil-foundation-pile-slab interaction. The method combines geotechnical requirements related to bearing capacity, settlement, and angular distortion with structural requirements by Upper Bound Theorem related to plastic rotations, bending moments, and crack control. The case studies demonstrate how soil–foundation–structure interaction principles can be applied in the rehabilitation of historic structures.

Keywords: Historic building foundations, plastic state of silty clay, jacked and spiral piles, upper and lower bound theorems of plasticity, spring coefficients of piles

INTRODUCTION

Strengthening and underpinning of historic buildings require a thorough understanding of both structural and geotechnical engineering, combined with practical experience gained through field investigations and construction activities.

The assessment process typically begins with a review of available historic drawings and documentation, followed by an estimation of the superstructure loads. After conducting a structural assessment and investigating the subsurface conditions, a preliminary engineering evaluation can be established. In most cases, however, only limited information regarding the structural system, its condition, and the foundation soils is available at the outset. Consequently, detailed site inspections are required to identify cracking patterns, structural tilting, and evidence of differential settlement.

The field observations are followed by analytical work, including load assessment and foundation calculations. Despite comprehensive geotechnical investigations, the estimated soil parameters may deviate from the mean values by more than 30% (Payne, 1995). Based on the collected information, preliminary design calculations are performed, often assuming that some foundation elements remain functional while others require underpinning and strengthening.

CASE STUDY: ALEXANDER STREET 10, FINLAND, HELSINKI

The building at Alexander Street 10 forms part of the historic building ensemble located at Alexander Street 4–10. The wing facing Helen Street 5 is also included within this ensemble (Figure 1A). The corridor of Helen Street, a three-storey house constructed in 1840, has continued to settle to the underpinning day in a 2 m thick silty clay layer.

The foundations of the building had been subjected to structural loading for more than 150 years, and consolidation of the underlying soils had been completed prior to the underpinning works carried out between 1991 and 1993. The subsoil conditions at the corner of Helen Street 5 and Alexander Street consisted predominantly of silty sand.

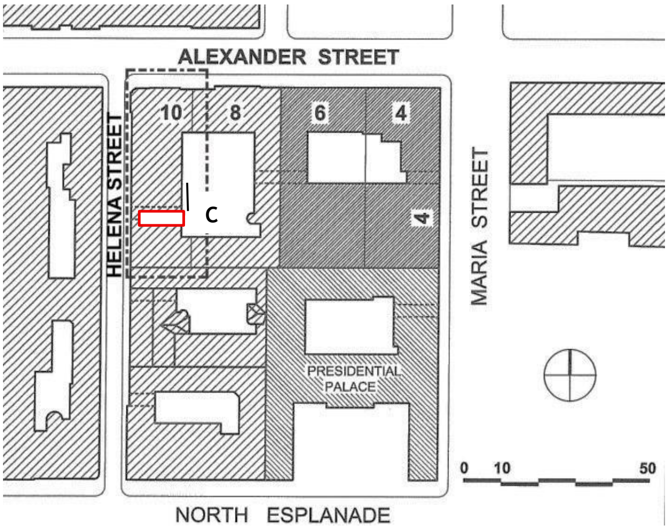

Figure 1A. *The buildings at Alexander Street and the corridor (C) to Helen Street 5.*

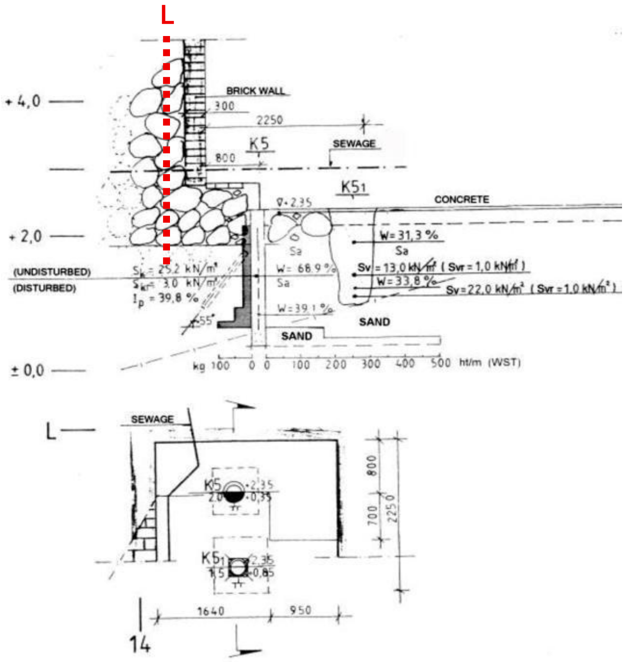

Figure 1B*. Corridor to Helen Street. Trial pit, Swedish weight sounding test (WST), vane test (Sv), shear strength (Sk) by fall-cone test.*

The study area is located within the post-glacial coastal deposits of southern Finland. The subsurface conditions are typical of former Baltic Sea environments, consisting of silty sand overlying layers of silty clay deposited during the post-glacial marine phase. Groundwater observations made during the investigation indicated a groundwater level approximately 1.0–1.5 m below the ground surface, varying seasonally. The trial pits and in-situ tests were positioned immediately adjacent to the existing corridor foundations and are therefore considered representative of the soil profile influencing the observed settlement behaviour.

The soil beneath the corridor facing Helen Street consisted of a silty clay layer underlying silty sand stratum. The contact pressure from the corridor superstructure was approximately 170–200 kN/m² on these strata. In-situ vane tests and laboratory tests as fall cone tests were performed in Pit K5 in line L next to corridor wall and Pit K5.1, located roughly 1 m apart (Figure 1B). The elevations shown in Figure 1B are expressed in metres relative to the local municipal height system, which approximately corresponds to mean sea level but is gradually changing due to ongoing land uplift.
Using the fall cone tests and the vane test results, neglecting horizontal loads and assuming the shear strength s_u and cohesion c to be the same, then the ultimate vertical bearing pressures outside the foundation are approximately in Pit 5 and Pit 5.1:

Pit 5, $q_u \sim 5.5 \times 25\ kN/m^2 + (0.5\ m \times 17\ kN/m^3) \sim 145\ kN/m^2$; Pit 5.1, $q_u \sim 80\ kN/m^2$ (1)

By using undisturbed sample of Pit 5.1 and CRS-test it was clear that the settlement process was still going and silty clay was settling in plastic state. The most demanding part of the project was the underpinning of the corridor foundations using concrete piers founded in sand (Figure 2A). Excavation was carried out manually, with removed soil lifted using small machinery (Figure 2B). Each pier place was stabilised by four drilled steel piles, one at each corner, acting as temporary support. The drilled steel piles used for temporary support were small-diameter steel piles (casings 139.7 x 4mm^2 and core steel d110mm). The piles were braced against buckling using welded steel plates, which also served as permanent formwork for concrete piers and were also designed to resist earth pressure. The core piles were drilled 2 m into the bedrock, subjected to test hammering to verify the pile toe bearing capacity, and then cement-grouted. Drilling records indicated competent rock suitable for pile installation.

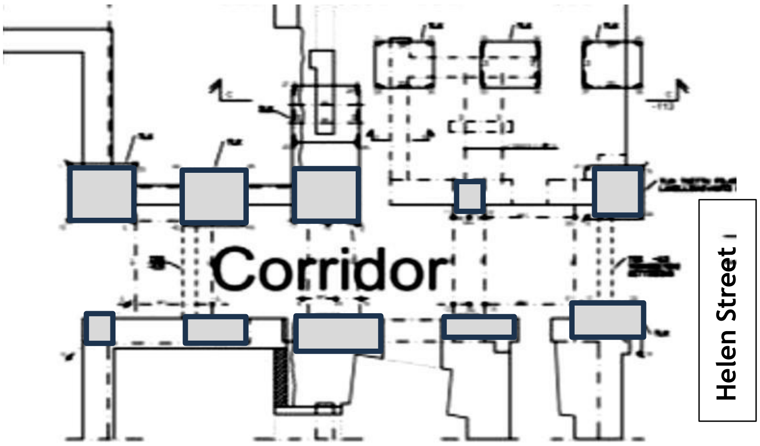

Figure 2A. *Overview of the corridor. Piers are dashed.*

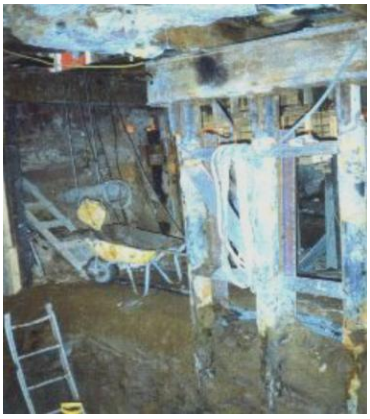

Figure 2B. *Picture of the underpinning corridor at Helen Street. All the concreate piers were jacked.*
Figure 3: *Picture of The Church before strengthening. The tower is visible, no roof, the shoring of walls.*

To prevent soil settlement, all the piers were jacked, the allowable upward movement was 1.5 - 2.0 mm. The testing time was 24 h and the leftover pretest load of the concrete pier was about 80% of the maximum load. The original block foundation is visible at the top of the (Figure 2B).

CASE STUDY: ST. JOHN'S CHURCH IN ESTONIA, TARTU

Construction of the masonry church is believed to have begun in the 13th century along with the western European crusaders. For Tartu (Dorpat), the city of Luebeck in Northern Germany, is believed to be the source of masonry development. A 16th-century account describes it as follows: "The church of John the Baptist, which is built with supreme artistic skill and great expense, and which, among other decorations, boasted the figures of the Saviour and the Twelve Apostles" (Bredenbach, 1558, *Peregrinatio in Terram Sanctam*).

During World War II, the church was severely damaged by fire and remained in ruins throughout the Soviet period, (Figure 3). St. John's Church in Tartu is unique within European Gothic architecture due to its extensive collection of more than one thousand terracotta sculptures and decorative elements, preserved both in the interior and on the exterior of the building. The overview of the Church before the WWII is illustrated in the Figure 4A.

Reasons and scope for strengthening of the foundations

The existing foundations of the church are on massive stones, which themselves were sitting on wooden rafts. The ground under the rafts consists of a variety of different soil layers. When ignoring the south-west part of the church which is lying on clay the main part of the church is lying on frictional soil. The approximate thicknesses of the soil layers under the wooden rafts are as given (Figure 4B). The one-dimensional consolidation of the loose sandy silt had been completed due age of the structure. The ground water level had sunk, and the building started to sink and rotting of the wooden rafts started, too. If the foundations had not been strengthened, the deterioration of the wooden rafts could have led to differential settlements exceeding 30 cm. The settlement map in the church area for the period from 1963-1987 is shown as contour lines (Figure 5A). The settlement as elevation levels over 16 years are shown in Figure 5B. The strengthening of the foundations of the tower was made during August 1993-February 1994 by step piling and pouring pile pads (Figure 6A). The result was that each pier was founded on its own floating piled raft. The other parts of the church ignoring collapsed and demolished part (Line B) and the liturgical spaces were underpinned by drilled and jacket spiral piles. The whole underpinning work was ready in 1996. The spiral piles were installed at both sides of the walls and at four sides of the columns. The spiral piles were jacked against concrete beams which were earlier pressed against existing foundations by VSL post tension strands (Figure 8A). Post tension strands were used to apply controlled prestressing forces between the new concrete beams and the existing masonry foundations. The jacking process, of the spiral piles, including both the pre-test and final load-stages (Figure 7), shifted the loads from the historic masonry structure onto the newly installed spiral piles, ensuring immediate load uptake with minimising any additional differential settlement.

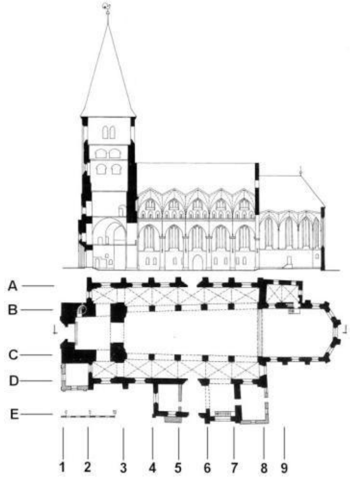

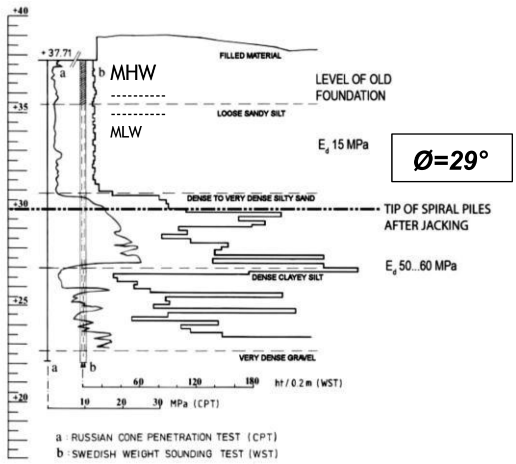

Figure 4A: *Plan and section before WW II.* ***Figure 4B:*** *Soil exploration results at sample point (Avellan 1996).*

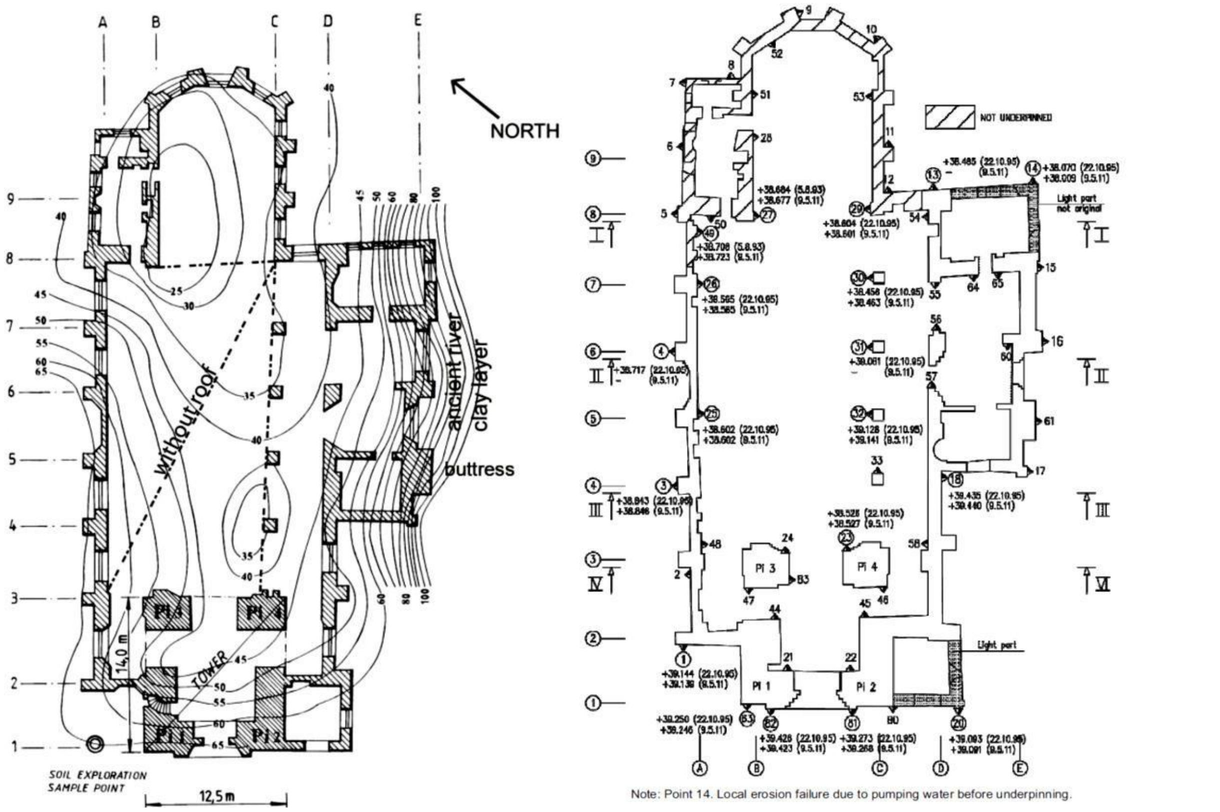

Figure 5A: *Settlement lines (mm) between years 1963-1987 without roof between lines A-B and 3-8 (Avellan & Lange 1997).* ***Figure 5B****: The settlement levels with the roof (m) for 16 years, 28.10.1995-9.5.2011.*

Underpinning of the Tower

The underpinning of the Tower of St. John’s Church was the first foundation strengthening project undertaken at the site. The original concept was to jack piles down to a dense gravel layer (Figure 4B). However, test piling revealed that the historic masonry structure was unable to withstand the localized compressive stresses generated by the jacking force of approximately 700 kN. As a practical engineering solution developed during construction, small floating piled pads were designed and installed sequentially beneath the tower supports. Together, these elements formed a floating piled raft foundation for each pier that provided additional support and load redistribution for each tower pier.

The weight of the Tower is 5500 tons it is supported by four piers Pi1-Pi4 (Figure 5A and 5B). Underpinning was carried out simultaneously beneath all piers, following a step-by-step sequence of jacking and concreting first the floating piled pads and then the floating piled rafts for each pier (Figure 6A). The bearing capacity of the work sequences were checked beforehand by logarithmic spirals.

Piling proceeded gradually by partly excavating stone masonry while simultaneously piling in the freed spaces. Jacked steel piles Ø 218 × 10 were used to strengthen the Tower. To ensure the stability of the structure, the piling work was scheduled in such a way that only one section of each pillar was set at one time. None of the pillars were installed completely at once, but all of them were under construction at the same time. The piling order was planned beforehand according to the settling and inclination measurements. The whole work was carried out with constant verification of measurements. In total 136 piles were installed below the underground extension of the tower, at approximately 0.8 m spacings. End-jacking procedure was performed with a load of 600...650 kN, which is 1.5 times the allowable maximum load of 400 kN.

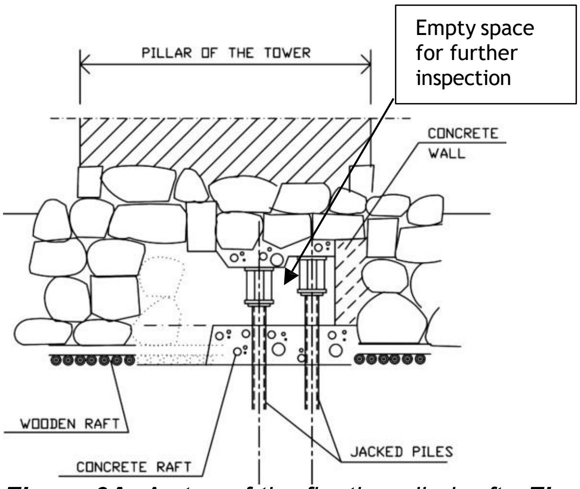

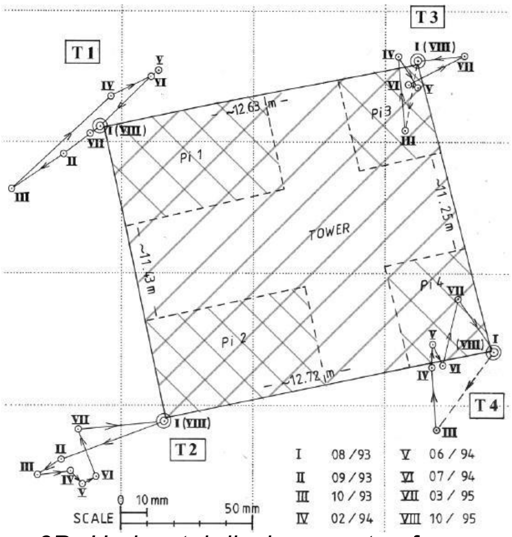

***Figure 6A**. A step of the floating piled raft.* ***Figure 6B:** Horizontal displacements of upper corners of the tower of St. John's Church at monitoring intervals (Avellan & Lange 1996).*

The rate of settlement and horizontal displacements of the tower were measured throughout the strengthening process. As a result of the construction technique, the overall settlement of the tower was only 18 to 20 mm (Figure 5B). At level 38 m from the ground surface level the horizontal displacements were 30…50 mm during the underpinning work (Figure 6B).

Underpinning of the Line A

The pile places for spiral piles were first opened by jetting and then the piles were embedded in the soil by twirling. The spiral piles were made of Φ218 x 10 and with spiral 25 mm c/c 180 mm. The joints of the spiral drilled piles were made by welding the parts together and twirling them. The piles were filled with concrete and jacked against concrete beam. The total length of the piles on axis A varied from 5.5 m to 6.5 m. A practical and simple technique and equipment was devised to enable the assembly of the spiral drilled piles by screwing in very limited workspaces. All the parts of the necessary equipment could be carried by workmen (Figure 8 B). The allowable load in SLS was 375 kN based on creep load 525 kN and the maximum used load was 360 kN. All the piles were pretested by a testing procedure of 180 min and then wedged (Figure 7).

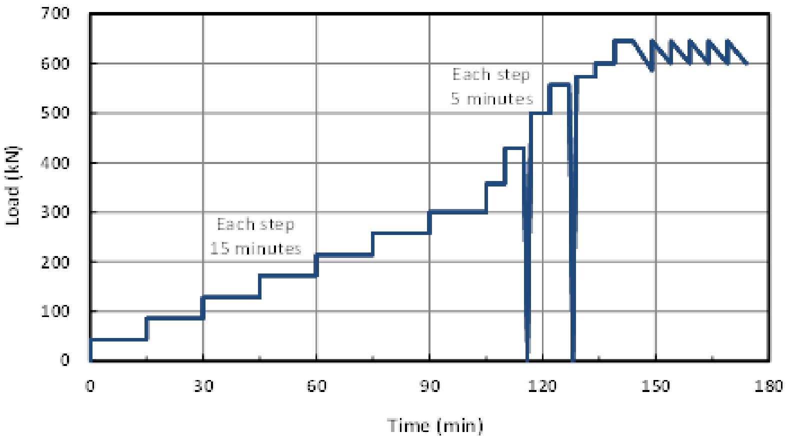

***Figure 7:** Time used for test loading of each of the drilled spiral piles in line A.*

LIMIT STATE DESIGN FOR FOUNDATIONS OF THE LINE B

The time to rebuild the Line B, (Figures 5A, 5B 49Aand 9B) occurred after underpinning the tower, outside, inside walls and interior piers which were underpinned by screw piles for stabilizing all the old structures.

The Line B refers to the longitudinal row of columns and arches located along the north-west side of the church nave (Figures 3A, 7 and 8). This part of the church was destroyed during World War II and was subsequently reconstructed. The reconstructed columns introduced additional vertical loads as well as eccentric loading effects arising from the asymmetrical arch configuration. The effective area, the shadowed area is 2.6 x1.71 m2 (Figure 9A).

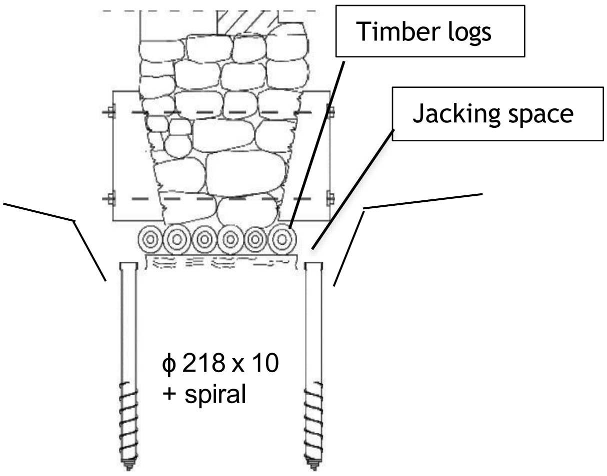

***Figure 8A:** Underpinning the wall by spiral piles. **Figure 8B:** Work pit for spiral pile. Picture of the drilling equipment and spiral pile.*

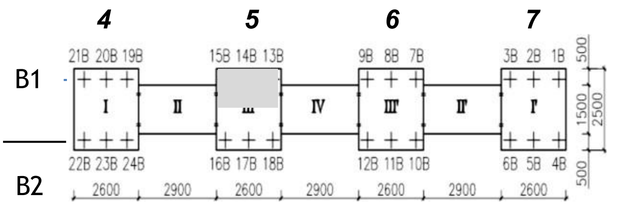

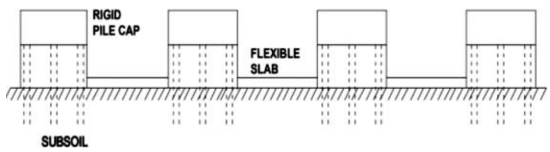

***Figure 9A**. Line B foundations overview and screw piles. **Figure 9B:** Line B section foundations and slabs.*

STRUCTURAL AND GEOTECHNICAL DESCRIPTION OF THE DESIGN METHOD

Avellan developed a simple design method for strip-foundations lying on frictional soil (Avellan 1992, 1994). The method shows how the strip foundation can be designed geotechnically and structurally by one method in ULS and SLS. The method uses lower and upper bound theorems of plasticity and was further developed for floating piled strip foundation and soil-foundation-pile interaction. Avellan (2011, 2015, 2019). The method may also be used for piled floating raft foundations by the idea of strip method (Hilleborg 1956).

A fundamental assumption of the Avellan Method is that the line of action of the resultant external actions remains unchanged between the Ultimate Limit State (ULS) and the Serviceability Limit State (SLS); only the magnitude of the resultant changes according to the applicable load combinations and partial factors. This assumption is consistent with the modelling approach adopted in Eurocode 7 for cases where the structural geometry and load-transfer mechanism are not significantly affected by geometric or material nonlinearity. As a result, the distribution of stresses and the overall structural behaviour can be evaluated using a common load path for both limit states.

The method may also be used to assess the geotechnical safety of historic buildings and monuments under changing loading conditions, such as nearby excavations, groundwater rise, and earthquakes. Separate foundations may be connected to new foundations between the old ones. The fixings can be done by dowels and chemical anchors.

Lower Bound Theorem and Upper Bound Theorem of Plasticity

Both fundamental theorems of plasticity—the Lower Bound Theorem (static theorem) and the Upper Bound Theorem (kinematic theorem)—are consistent with and implicitly accepted by the limit-state design philosophy of Eurocode 0, Eurocode 2, and Eurocode 7.

The lower bound theorem of limit analysis has been widely used and established in the literature on plasticity theory. Particular in soil mechanics, Chen (1975) and Salençon (2001) provide classical and foundational treatments of the static (lower bound) approach, demonstrating its applicability in soil mechanics in determining safe collapse loads by constructing statically admissible stress fields that do not violate yield criteria. The lower bound theorem has been extensively applied by subsequent Authors in both soil and structural engineering contexts. The lower bound theory of reinforced concrete slabs was first produced by Arne Hillerborg (Hillerborg 1956) and the theory can be used for beams and frames too.

The upper bound theorem of limit analysis has been widely used in structural engineering. The kinematic mechanism methods application, yield line theory of reinforced concrete slabs has been used worldwide after the WWII (Johansen 1943) and the theory for beams and frames especially for steel structures is commonly used.

Elastic-plastic model of frictional soil and spring coefficient of piles

Horn (1972) made horizontal full-scale tests in frictional soil for horizontal movement and horizontal passive pressure. He found the relationship between the ratio $P_p(s)/P_p$ and S/S_f to be non-linear (Figure 10). Avellan noticed by formula (3) and Figure 10 that vertical ultimate contact pressure of shallow foundation is mainly depending on passive pressure and the movement is settlement. Then Avellan used for frictional soils elastic-plastic model, which is based on pressure-settlement relationship implicating elastic behaviour up to the ratio S/S_f (settlement/settlement at failure) = (0.20) 0.18. For this settlement ratio the passive pressure Pp(s) is (0.70) 0.625 times the passive pressure at failure Pp and 1/1.6 (1.43) = 0.625 (0.70) (Figure 10).

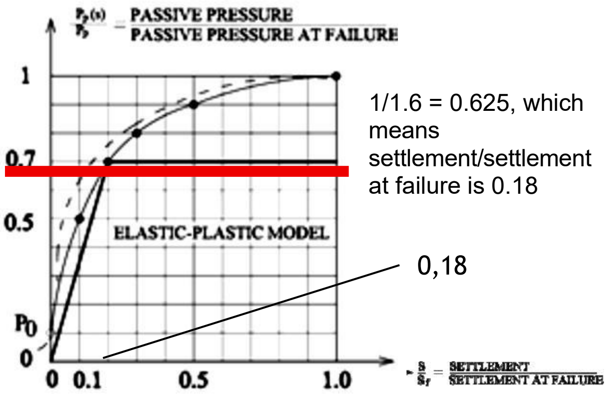

Figure 10. Elastic-plastic model according to the Author and based on the investigation of (Horn 1972, Avellan 1992).

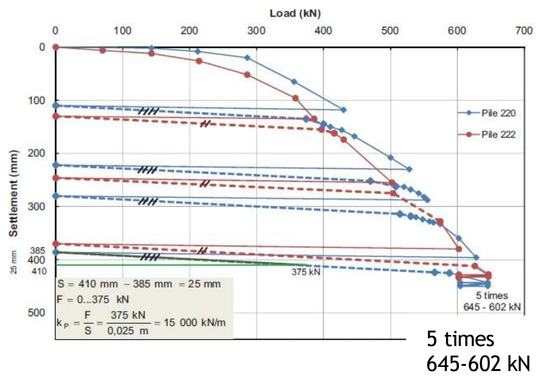

Figure 11. Spring coefficients of tested piles on the line A (Avellan 2011).

The strict line shown in Figure 10 should be regarded as project-specific engineering model for frictional soils. The settlement can be predicted using different methods, like Schleicher (1926), elastic theory and Schultze & Sherif (1973) empirical measurements, both used by Avellan (1992, 2011). The methods require soil investigations, such as the Swedish Weight Sounding Test (SWT), Cone Penetration Test (CPT), Standard Penetration Test (SPT), and representative soil samples, to obtain best-estimate values of the deformation modulus and the friction angle. The primary purpose is to assist in the design of concrete foundations on frictional soils for the GEO and STR limit states. To support this objective, the method provides a rational framework for estimating the relationship between foundation contact pressure and foundation settlement (Figure 10). The load–settlement diagram shown in Figure 11 is applicable only to the piles tested and the soil conditions at St. John's Church.

The same contact pressure in ULS and SLS

All the design values in the SLS can be calculated by dividing the USL values by $\gamma_{t,a}$, owing the linear or nearly linear behaviour of ground model (substructure model) (Figure 10).

The total safety factor of actions of $\gamma_{t,a}$ which is the sum of design actions (F_d) in ULS divided by the sum of actions (F_k) in SLS and is a simple and useful tool between those limit states $\gamma_{t,a}$:

$$\gamma_{t,a} = \Sigma F_d / \Sigma F_k \tag{2}$$

$$\text{USL} \quad p_d \leq \Sigma F_d / A_F \tag{3}$$

$$\text{SLS} \quad p_k \leq \Sigma F_k / A_F = (F_d / \Sigma \gamma_{t,a}) / A_F \tag{4}$$

p_d is the design value of contact pressure from the superstructure,
p_k is the characteristic value of contact pressure from the superstructure,
A_F is the effective area of the foundation

Structurally, the method complies with EC-2 and incorporates the upper- and lower-bound theorems of plasticity (Avellan 1992, 2011, 2015). The plastic bending moments of the foundation are determined using the upper-bound theorem through the kinematic approach. Geotechnically, the method employs the same contact pressure p_d in both SLS and ULS, thereby satisfying the safety requirements against ground failure.

The ultimate failure pressure q_u for each part of foundations can be calculated using acceptable bearing capacity formulas. The design pressure q_d is:

$$p_d \leq q_d = q_u / \gamma_{R,v} = q_{ultimate} / 1.6 \tag{5}$$

q_u is the ultimate soil pressure, at failure,
q_d is design value of contact pressure from the substructure

The ultimate bearing capacity, q_u can be estimated using well-established bearing capacity equations, such as those proposed by Brinch Hansen (Brinch Hansen, 1961). The value ($\gamma_{R,v} = 1.6$), adopted by Avellan (1992, 1994, 2011), is based on the observation that the relationship between horizontal pressure and horizontal displacement is linear, or nearly linear, up to a pressure ratio of 0.625 (Figure 10). The bearing capacity of shallow foundations is fundamentally governed by passive earth pressure. The bearing capacity factor N_q is derived from passive earth pressure theory, and the remaining bearing capacity factors are expressed as functions of N_q. According to Reissner (1924), N_q is given by:

$$N_q = K_p \, e^{\pi \times \tan \Phi} \tag{6}$$

The "real settlement" in SLS is the calculated settlement in ULS divided by $\gamma_{t,a}$

Assuming partial factors γ_g as 1.35 (permanent actions, dead load) and γ_g as 1.50 (variable actions, live load) of the superstructures we get as $\gamma_{t,a}$ (2).

$q_k / g_k = 0.5$, then $\gamma_{t,a}$ is 1.40 and used for St. John's church
$q_k / g_k = 1.0$, then $\gamma_{t,a}$ is 1.425

The flowchart for the Method

The method takes the following into account as geotechnical requirements: contact pressure, total settlement and angular distortions; and as structural requirements; admissible plastic rotations, end moments due to displacement angle, as well as control of cracking. The procedure for geotechnical and structural design in both limit states for strip foundation is shown as a flowchart in Figure 12 (Avellan 1992, 1994, 2011, 2015).

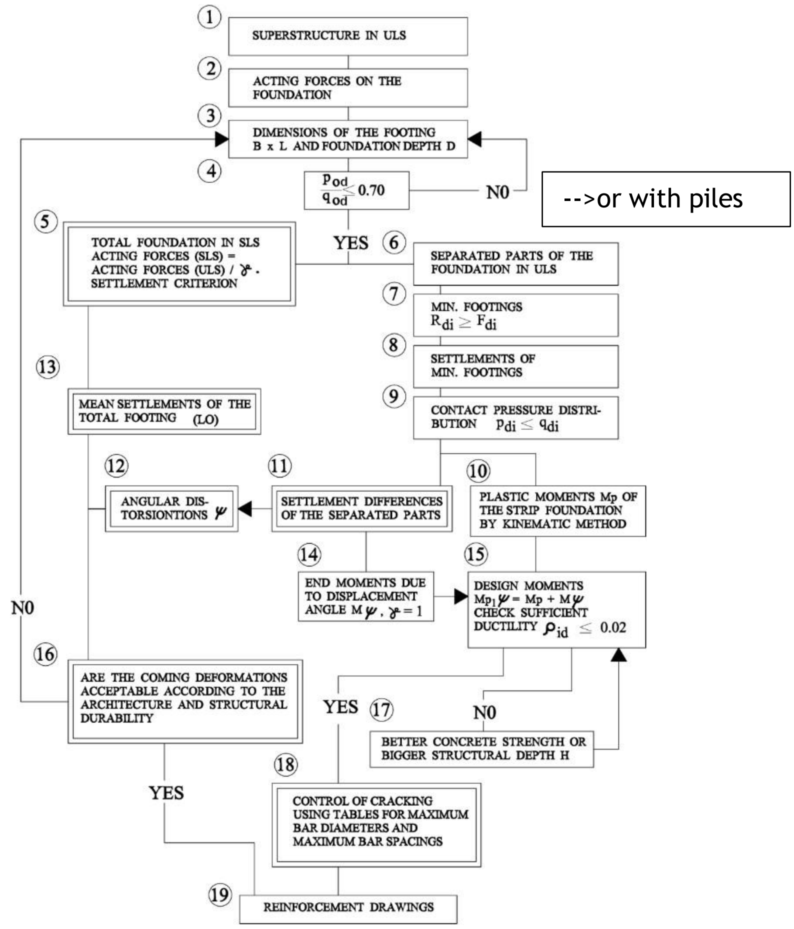

Figure 12: *Geotechnical and structural design procedure in limit states for strip foundation. Double lines around boxes represent serviceability state. $p_o=p_{od}$ is mean design contact pressure calculated from superstructure beneath the whole strip foundation. $q_o=q_{od}$ is the mean resistance contact pressure of substructure beneath the whole strip foundation. The value 0.7 in the box 4 is later reduced to 0.625.*

The use of flowchart:
Boxes 1-3, The design procedure starts with the total foundation
Box 4, If the mean contact pressure of USL actions of superstructure divided by the mean contact pressure of the resistances of substructure is less than 0.7 (0.625) then go further. If no, then new dimensions of the foundation or piles. The following boxes are due to Axioms 1-4.

The geotechnical design process of the flowchart is simply underpinned by Lower Bound Theorem:

The lower-bound condition is (design contact pressure from the superstructure) $p_d \leq q_d$ (design contact pressure from the substructure) and

- If $p_d < q_d$→ the foundation is safe
- If $p_d = q_d$→ the system is exactly at the limit state
- If $p_d > q_d$→ failure occurs (not allowed in ULS)

This can be formulated for strip foundations simply; the geotechnical limit state design of a strip foundation by lower bound theory can be performed using axioms 1 to 4, (Figures 13-17) (Avellan 1992, 2011).

<u>*Axiom 1:*</u> All individual parts in the loaded strip foundation can be designed independently of other parts, representing thus a minimum foundation to meet the requirements for the design in ULS (Figures 13-14).

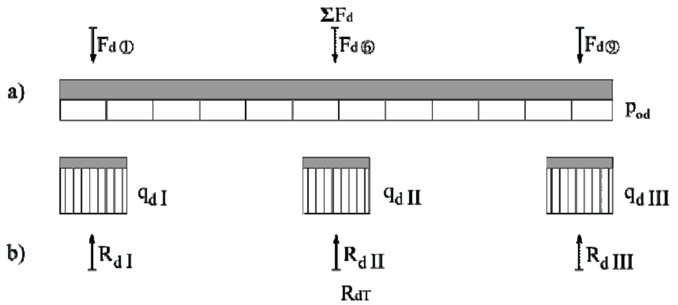

Fd (1) ≤ Rd (1)
Fd (6) ≤ Rd (2)
Fd (9) ≤ Rd (3)

***Figure 13**: a) Strip foundation, design loads, and design contact pressure of superstructure.*
*b) Separate parts, resistant contact pressures, and resistances of substructure (*Avellan 2011).

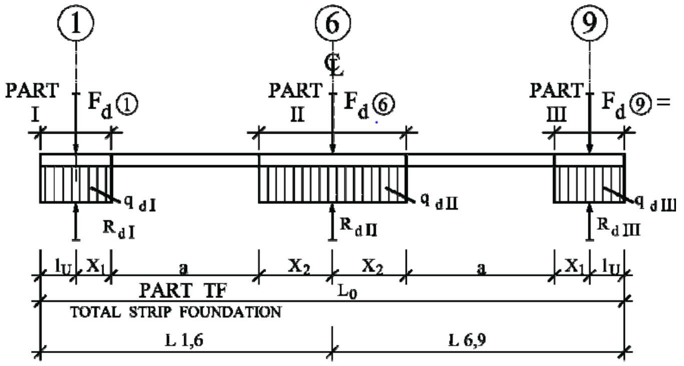

***Figure 14:** Total strip foundation and separated minimum parts I, II, III. Forces acting in ULS (Fd) from the superstructure and opposing forces R_d. (*Avellan 1992).

<u>*Axiom 2:*</u> The resistance (R_{dT}) of the whole strip foundation is not less than the sum of the resistances in individual parts (Figure 14).

R_{dT} ≥ Rd (1) + Rd (2) + Rd (3).

Thus, the failure capacity of the soil for the whole strip foundation is verified by the individual parts of the strip foundation considered separately.

<u>*Axiom 3:*</u> Distribution of contact pressure shall satisfy the requirements of equilibrium in all individual parts and the mean contact pressure due to loads (p_{od}) shall not exceed the mean design contact pressure of substructure (q_{od}).

The distribution of contact pressure for the ULS analysis can be taken into account of by choosing contact pressures (p_d) according to the following conditions which means that the lower bound theorem becomes fulfilled in the ULS in the simplest way for the minimum effective foundation, i.e. $p_d \leq q_d$, (Figure 15).

p_d (1) ≤ q_d (1)
p_d (6) ≤ q_d (6)
p_d (9) ≤ q_d (9)

In addition, the distribution of the contact pressure p_d (x) must be applied in such a way that the mean contact pressure is p_{od} in Figure 16 (Avellan 1992).

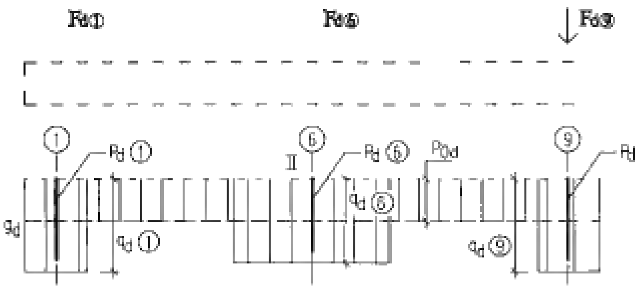

***Figure 15**. Contact resistance pressure q_d of parts I, II and III and contact pressures p_d of parts I, II, III. The mean contact pressure p_{od} of total foundation (TF) (*Avellan 1992).

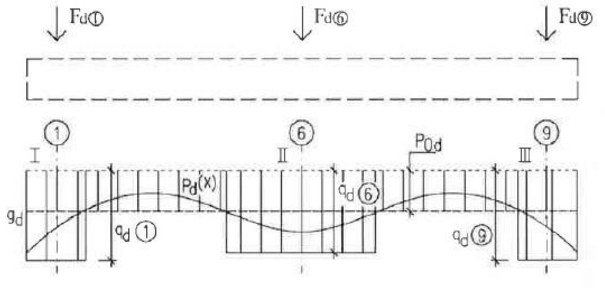

***Figure 16**: Balanced contact pressure $p_d(x)$ (Avellan 1992).*

<u>*Axiom 4*</u>: The settlement of the total strip foundation is less than the sum of the settlements of the parts in the foundation.

The relative values of the settlements in relation to the settlement of the total strip foundation are shown in (Figure 17) and the settlement of the total strip foundation, denoted as TF, is less than the sum of the settlements of foundation I, II and III.

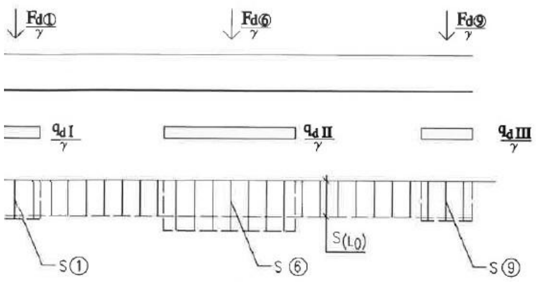

***Figure 17**: Relative settlements of parts I, II, III and total foundation (TF) when the settlement TF (S(L0)) is given a unity value (Avellan 1992).*

Structurally, the method complies with EC-2 and incorporates the upper- and lower-bound theorems of plasticity (Avellan 1992, 2011, 2015). The plastic bending moments of the foundation are determined using the upper-bound theorem through the kinematic approach.

SHORT NUMEROUS CALCULATIONS

Design in Line B

First the design calculation starts with soil-foundation-pile interaction. Characteristic loads in SLS (V_{kP}) were multiplied by a total safety factor, $\gamma_{t,a}$ (=1.4) for design loads in ULS (V_{dP}). The γ_{ta} is based on partial factors of live and dead load. The load for each foundation was characteristic load V_{kP} 1104 kN and design load V_{dP} 1546 kN. Because of rebuilding arches, the structural eccentricity from piles Line B2 is 0.394 m, the rand distance is 0.5 m, and then the effective bread of the on-ground laying foundation is 1.71 m dashed area (Figure 9A). The design load having safety factor for piles 1.1 was:

415 kN/1.1 = 377 kN and in SLS 415 kN/1.40 = 300 kN (7)

The piles were finally tested by 5 load steps (415-450 kN). The same testing procedure with greater loads was used on the line A, and the load - settlement diagram for special pretested piles is shown (Figure 11, Avellan 2011).

Soil foundation pile interaction in SLS

According to Brinch-Hansen (1961), the q_u is 173 kN/m^2 for the foundation (B x L x D) = (1.71 x 2.6 x 0.3) m^3.

$$q_d = q_u/1.6 = 108.4 \text{ kN / m}^2 \tag{8}$$

By Schleicher (1926) modified by Tsytovich (1981) the calculated settlement of foundation S_F is 9.7 mm having E_d as 15 MPa (Figure 4B). The spring coefficient (k_F) for foundation is 49 685 kN/m. The spring coefficient for free piles (Σk_P) is 45 000 kN/m (Figure 11). The Q_F is the reaction force of the foundation.

Compatibility equations in SLS are equations 7 and 8. The equations for USL are the same, but instead, for ULS calculations, design values (subscript d) are used instead of characteristic values (subscript k).

$$\begin{cases} S_F = S_P \\ Q_F + \Sigma F_{kP} = V_{kP} \end{cases} \tag{9}$$

$$\begin{cases} S_F = \dfrac{Q_F}{k_F} \\ S_{kP} = \dfrac{\Sigma F_{kP}}{\Sigma k_P} \end{cases} \tag{10}$$

SLS: The pile load F_{kP} is 174.9 kN < 300 kN and the settlement of the piles is S_P 11.7 mm, and the settlement of foundation S_F is the same. The ultimate settlement S_{Fu} according to Figure 10 is 54 mm (9.7 mm/0.18), and the ratio S_F/S_{Fu} is 0.22 and then q_{kF} (ground pressure under foundation) is 0.72 times q_u (Figure 10, non-linear line). This means q_{kF} is 124.8 kN/m^2 and safety factor γ against soil failure is 1.39, but piles have capacity enough.

USL: F_{dP} is 244.9 kN < 377 kN, and $S_F = S_P$ = 16.3 mm. The ratio S_F/S_{Fu} = 0.30 and q_{df} =138.7 kN/m^2. The safety factor γ against soil failure is 1.25, however, piles have resistance enough. If the soil resistance is 0, then the piles up 19B to 21B (Figure 9A) have pile loads 374 kN (and settlements 24.9 mm) and piles 22B up to 24B pile loads 141.7 kN (and settlements 9.4 mm). The design check having soil resistant as 0 is also suggested by Viggiani et al. (2012).

The calculations indicate that both serviceability and ultimate limit state requirements were satisfied. The analysis also demonstrates that the piles provide a substantial reserve capacity should the contribution of the supporting soil decrease over time.

Soil-foundation-pile-slab interaction

The design procedure follows the procedure according to flowchart (Figure 12). Detailed design calculation is described in Avellan (2011). Using the axioms which are explained in text with figures 13-17 we get the contact pressure the q_d and p_d (x) curves (Figure 18B).

Plastic bending moments of slab II

The contact pressure distribution and calculation procedure for plastic moment distribution are exemplified (Figure 18). It provides an illustration of a practical application from Tartu, Estonia. By incorporating the external (W_e) and internal virtual work (W_i), we get:

$W_e = W_i$

$\Sigma\, dF_d\, dz = \Sigma\, i\, M_p\, \varphi$ (11)

Mp is plastic bending moment;
i is the ratio of the negative plastic bending moment to the positive plastic bending moment. According to EC2, the value of i should be between 2.0 and 0.5;
φ is the rotation;
dF_d is design value of action;
dz is virtual displacement of action.

The practical manner to calculate plastic bending moments of slab II is by iteration (Figure 18C).

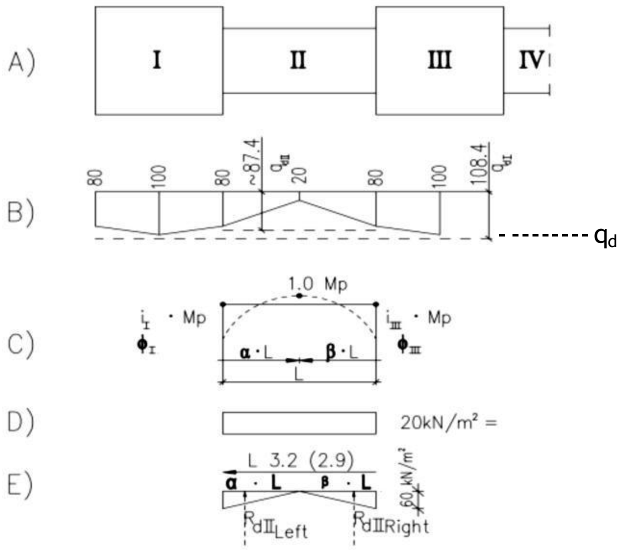

Figure: 18 *A) Structural system seen from the top. B) Contact pressure $p_d(x)$ under the structure. C) Slab II. Plastic moment distribution. α, β = left and right partial span ratio. D) Slab II: Contact pressure, uniformly distributed part. E) Slab II: Contact pressure, triangularly distributed part and its resistances (Avellan, 2011).*

The design calculation goes further using the structural design procedure according to the Figure 12. The calculation used the same procedure as equations 7 and 8. The results in the SLS are:

The settlement of foundation I, (S_F) SLS is 11.1 mm and in foundation II is 10.2 mm. The differential settlement is 0.9 mm, and the angular distortion is 1/3721. The small bending moment from angular distortions can be calculated. The influence of the flexible slab is for foundation I, 11.7 mm -11.1mm = 0.6mm and for foundation III, 11.7mm-10.2mm = 0.5mm.

The rigid piled floating pads take the loads, and the slabs have no practical influence. The measured SLS settlements of the line A are between 1-3 mm and the calculated SLS settlements of the Line B without slabs are 11.7 mm, and with slabs the settlement for foundation FI is about 10.9 mm and foundation FII about 10.1 mm. This shows that non-rigid slabs have a small or no effect on settlements (Figure 9B).

CONCLUSIONS

Geotechnical and structural design, as well as construction work involving historic buildings, require continuous engineering assessment and, in many situations, rapid professional judgement based on limited information and observations made during construction.

The corridor along Helen Street had continued to settle up to underpinning date within an approximately 2 m thick silty clay layer. The observed settlement was not caused by primary consolidation; rather, the silty clay remained in a plastic state and continued to deform under essentially constant effective stress. In 1991, this behaviour was not widely recognized in Finnish geotechnical practice. The case demonstrated that silty clay may exhibit long-term plastic deformation without significant changes in effective stress.

The foundation of the Tower was underpinned step by step with pretested jacked piles and a concrete raft poured step by step. The walls and columns of St. John’s Church was carried out using spiral piles. As a technical lead and principal designer of the whole underpinning, the Author visited the site regularly to provide technical guidance, supervise critical construction activities, and advised the contractor. The rebuilt foundation along Line B was constructed in accordance with the Author's design drawings and design method.

The design method assumes the same soil pressure distribution ($p_d \leq q_d$) in both the Ultimate Limit State (ULS) and the Serviceability Limit State (SLS), allowing the substructure to be designed using a single calculation procedure. The method is based on strip foundations on frictional soils and follows the Lower Bound Theorem of Plasticity using Axioms 1–4. Design bending moments for reinforcement are determined using Upper Bound Theory, while end moments resulting from structural displacements are added to the calculated design moments.

Both fundamental theorems of plasticity—the Lower Bound Theorem (static theorem of plasticity) and the Upper Bound Theorem (kinematic theorem of plasticity)—are consistent with the limit-state design philosophy of Eurocode 0 (Basis of Structural and Geotechnical Design), Eurocode 2 (Design of Concrete Structures), and Eurocode 7 (Geotechnical Design). The Eurocodes permit and, in several design methods, implicitly employ concepts derived from these theorems, although the theorems themselves are not explicitly presented.

The method may also be used to assess the geotechnical safety of historic buildings and monuments under changing loading conditions, such as nearby excavations, groundwater rise, and earthquakes. Separate foundations may be connected to new foundations between the old ones. The fixings can be done by dowels and chemical anchors.

A resistance factor of $\gamma_{R,v} = 1.6$ for soil bearing pressure at failure implies that the relationship between soil pressure and settlement remains fully, or approximately, linear within the design range. The value recommended in Eurocode 7, $\gamma_{R,v} = 1.4$, is lower and may result in conditions where the soil pressure–settlement relationship becomes non-linear. Upper- and lower-bound plasticity principles are applied to evaluate structural response and soil pressure distribution, while elastic–plastic soil behaviour and pile spring coefficients are used to quantify load sharing among the soil, piles, and superstructure. Practical applications of the method are presented in Avellan (1992, 1994, 2011, 2013, 2015).

Monitoring data provide important validation of the adopted design approach. Settlement measurements collected between 1995 and 2011 indicate that post-strengthening movements remained small and generally consistent with design predictions. Measured settlements of the strengthened structures were in the acceptable limits in SLS.

REFERENCES

Avellan, K. (1992). Licentiate Thesis in Finnish: Geotechnical and Structural Ultimate Limit State Design of Foundations Resting on Soil. Helsinki University of Technology, Faculty of Civil and Environmental Engineering (p. 258).

Avellan, K. (1994). Ultimate Limit State Design of Strip Foundation. In Proc. 13th ICSMGE, New Delhi pp. 449-452

Avellan, K. & Lange, K. (1996). St. John's Church, Tartu, Estonia – Underpinning of tower. In Viggiani C (Edit.) Geotechnical Engineering for Preservation of Monuments and Historic Sites. Proceedings of the International Symposium on Geotechnical Engineering for the Preservation of Monuments and Historic Sites. Naples, 3–4 October 1996. Rotterdam, Balkema: 521–525.

Avellan, K. (2011). Limit state design for strengthening foundations of historic buildings using pretested drilled spiral piles with special reference to St. John's Church in Tartu. Doctoral thesis. (University of Oulu, Faculty of Technology, Department of process and environmental Engineering).

Avellan, K. (2013) Limit state design for strengthening the foundations of St. John's church of Tartu, Estonia using pretested drilled spiral piles". International Conference on Soil Mechanics and Geotechnical Engineering (18th ICSMGE), Paris, France 2.- 6.9.2013 Palais des Congrès.

Avellan, K. (2015). Simple calculation method for soil-foundation-pile slab interaction. 16th European Conference on Soil Mechanics and Geotechnical Engineering (ECSMGE), Edinburgh, Scotland, 13th – 17th September 2015.

Avellan, K. (2019). The impact of partial factors on the design of foundations for precast concrete structures. Proceedings of the XVII ECSMGE-2019, Reykjavik.

Bredenbach, T. (1558). Peregrinatio in Terram Sanctam. Cologne.

Brinch-Hansen, J. (1961). A general formula for bearing capacity. Copenhagen. Akademiet for de tekniske videnskaber Geoteknisk institute. Bulletin no. 11: 38–46.

Chen, W.F. (1975). Limit Analysis and Soil Plasticity. Elsevier.

European Committee for Standardization (CEN). (1990). *EN 1990:2002 Eurocode – Basis of Structural Design*. Brussels: CEN.

European Committee for Standardization (CEN). (2004). Eurocode 2: Design of Concrete Structures – Part 1-1: General Rules and Rules for Buildings (EN 1992-1-1). Brussels: CEN.

European Committee for Standardization (CEN). (2004). Eurocode 7: Geotechnical Design – Part 1: General Rules (EN 1997-1). Brussels: CEN.

Hillerborg, A. (1956). Equilibrium theory for reinforced concrete slabs (in Swedish). Betong 1956. 171-182.

Horn, A. (1972). Resistance and movement of laterally loaded abutments. *Fifth Eur Conf on Soil Proc*, 143-148, Madrid, Spain.

Johansen K.W. (1943 & 1962) Yield-Line Theory. Cement and Concrete Association, London.

Payne, I. (1995). Report on the ICE Ground Board Piling and Ground Treatment Panel meeting "Aspects of soil structure interaction" ICE 13th July 1994. Ground Engineering January/February 1995.

Reissner, H. (1924). *Zum Erddruckproblem.* In: Proceedings of the First International Congress for Applied Mechanics, Delft, The Netherlands, C. B. Biezeno & J. M. Burgers (eds.), J. Waltman Jr., Delft, pp. 295–311.

Salençon, J. (2001). The Static and Kinematic Methods of Limit Analysis in Soil and Rock Mechanics. Springer.

Schleicher, F. (1926). Zur Theorie des Baugrundes. Der Bauingenieur. Heft 48: 931–935, Heft 49: 949–952. (The theory of the ground. The Civil engineer. Block 48:931–935, Block 49, 949–952.)

Schultze E. & Scheriff G. (1973). Prediction of settlements from evaluated settlement observations for sand. Moscow. Proceedings of the eighth ICSMFE: 225-230.

Tsytovich N (1981) Soil Mechanics. Moscow. English translation Mir Publisher.

Viggiani C. et al. (2012). Piles and Pile Foundations. ISBN: 978-0-203-88087-6. Taylor & Francis, London & New York.